Nature of Ferroelectricity in KNO_3†

ARTHUR CHEN*‡ AND FRED CHERNOW§
Department of Electrical Engineering, Massachusetts Institute of Technology, Cambridge, Massachusetts
(Received 6 July 1966; revised manuscript received 4 November 1966)

The lattice parameters of KNO_3 were measured in the temperature region of the ferroelectric transition. The changes in the lattice parameters as the crystal undergoes the paraelectric-to-ferroelectric transition have been interpreted as being due to the electrostriction effect. The dielectric constants and losses along the ferroelectric axis have been measured in the audio, megacycle, and microwave frequency regions. The occurrence of a relaxation type of dielectric dispersion in the microwave region, together with the contraction of the ferroelectric axis at the transition, suggests that ferroelectricity in KNO_3 is an order-disorder phenomenon. The observed first-order ferroelectric transition is caused by the large lattice-dipole coupling. A statistical theory based on a double well potential for the nitrate ion and on the assumption of a lattice-dependent internal field explains the origin of the electrostriction effect and the observed anomalies of the ferroelectric transition. The statistical theory is related to Devonshire's thermodynamic theory of the ferroelectric transition, and good agreement is obtained between the theoretically predicted and the experimentally determined coefficients of Devonshire's free energy.

I. INTRODUCTION

RECENTLY Sawada *et al.* discovered that KNO_3 in one of its polymorphic forms exhibits ferroelectric properties along one of its crystallographic axes.[1] The dielectric constant along the trigonal axis measured at 100 kHz showed a typical Curie-Weiss behavior in the paraelectric phase, and hysteresis loops were observed in the ferroelectric phase. The ferroelectric transition at 125°C is a first-order transition. Associated with this transition[2] are a volume change and a latent heat.

The present investigation was undertaken to determine the nature of ferroelectricity in KNO_3 and to explain the observed anomalies associated with the ferroelectric transition. We have measured the change in lattice parameters of KNO_3 as it passes through the ferroelectric transition. In addition, the dielectric constants and losses along the ferroelectric axis were measured in the audio, megacycle, and microwave frequency regions. The far-infrared reflectivity of the paraelectric phase of KNO_3 was also determined. The conclusion is that ferroelectricity in KNO_3 is an order-disorder phenomenon in which the first-order ferroelectric transition is caused by a strong lattice–electric dipole interaction. A statistical and thermodynamic theory was developed to explain the observed anomalies of this transition.

II. BACKGROUND

The existence of these polymorphic forms of KNO_3 was established by Bridgman in his studies on the effect of high pressure on univalent nitrates.[2] The phase diagram of KNO_3 as measured by Bridgman is shown in Fig. 1. Phase III, the ferroelectric phase, is a metastable phase at atmospheric pressure with a temperature range of 10–20°C. It always appears when the crystal is cooled from above 180°C, but does not appear when the crystal is heated from Phase II.

The structures of the various phases of KNO_3 were studied prior to the discovery of ferroelectricity in Phase III.[3–5] The structure of Phase I, the paraelectric phase, is closely related to the calcite structure.[3] It belongs to the space group D_{3d}^5-$R\bar{3}m$ and has one molecule per unit cell. From the projected electron density, Tahvonen suggested that the nitrate ion is oscillating along the c axis with an amplitude of about 0.4 Å. The structure of the ferroelectric phase is closely related to that of the paraelectric phase belonging to the space group C_{3v}^5-$R3m$; however, in this phase the nitrate ion is known to be displaced along the c axis from the center of the unit cell by ~0.5 Å.[4]

Phase II, which has no unusual dielectric properties, has the aragonite structure.[5] The Phase II → Phase I transition is of the so-called reconstructive transformation. We shall not be concerned with this transformation in the present studies.

Based upon the above structure analysis, Sawada, Nomura, and Asao have proposed the following model for ferroelectricity in KNO_3.[6] In the paraelectric phase the nitrate ion is oscillating along the c axis. In the ferroelectric phase, there exists a potential barrier in the center of the unit cell which hinders the oscillation of the nitrate ion. The spontaneous polarization P_s is then simply related to the displacement δ of the nitrate ion from the center of the unit cell by

$$P_s = Nq\delta, \tag{1}$$

† This research has been supported by the Electro-Tec Corporation, Ormond Beach, Florida.
* This work is based in part on a thesis submitted to the Department of Electrical Engineering at the Massachusetts Institute of Technology in partial fulfillment of the requirements for the degree of Ph.D.
‡ Present address: General Electric Research and Development Center, Schenectady, New York.
§ Present address: Department of Electrical Engineering, University of Colorado, Boulder, Colorado.
[1] S. Sawada, S. Nomura, and S. Fujii, J. Phys. Soc. Japan **13**, 1549 (1958).
[2] P. W. Bridgman, Proc. Am. Acad. Arts Sci. **51**, 579 (1916).
[3] P. E. Tahvonen, Ann. Acad. Sci. Fennicae, Ser. AI **44**, (1947).
[4] T. F. W. Barth, Z. Physik. Chem. (Leipzig) **B43**, 448 (1939).
[5] D. A. Edwards, Z. Krist. **80**, 154 (1931).
[6] S. Sawada, S. Nomura, and Y. Asao, J. Phys. Soc. Japan **16**, 2486 (1961).

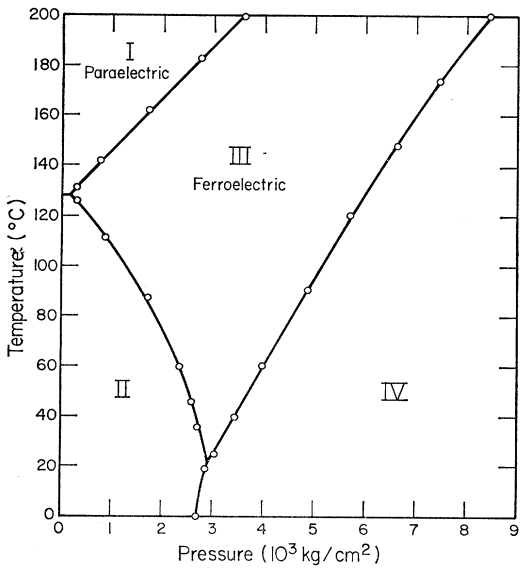

FIG. 1. Phase diagram of KNO_3 [after Bridgman (Ref. 2)].

where N is the number of dipoles per unit volume. Assuming q to be a unit electronic charge for the nitrate ion and using the measured $\delta=0.55$ Å, the resultant polarization is 11 μC/cm^2. This compares favorably with 8 μC/cm^2 and 10 μC/cm^2, as determined by hysteresis-loop and pyroelectric measurements, respectively.[6]

The structure of the paraelectric phase can also be interpreted as due to the disordered displacement of the nitrate ions from the centers of the unit cells. In this phase Shinnaka has observed by x ray six satellite peaks about the reciprocal-lattice point (111) and has interpreted these satellites as due to the disordered arrangement of the nitrate ions.[7]

Recently Yanagi and Kawabe have completed a study of the infrared spectra (600–1900 cm^{-1}) of KNO_3.[8] In addition, they have also measured the changes in the lattice parameters of the $K_{1-x}Rb_xNO_3$ and $K_{1-x}(NH_4)_xNO_3$ systems.[9]

III. LATTICE PARAMETERS MEASUREMENT

The theory of accurate lattice parameter measurement utilizing the x-ray diffractometer has been derived by Wilson.[10] The fractional error in the measured d spacing is given by

$$\frac{\Delta d}{d}=\left[\frac{1}{2\mu R}+\frac{A^2}{3R^2}\right]\cos^2\theta+\frac{S}{R}\cos\theta\cot\theta. \qquad (2)$$

The first term is the error caused by x-ray absorption and by the lateral misalignment of the sample. The second term is the error caused by the perpendicular displacement of the flat sample surface from the axis of rotation of the diffractometer. As the relative contribution of the two terms is unknown, the largest observable 2θ diffraction peaks were used to minimize the difference between $\cos^2\theta$ and $\cos\theta\cot\theta$ extrapolation procedures. To obtain the observable lines at large 2θ, large diffractometer slits together with Fe$K\alpha$ radiation and low scanning speed were used.

TABLE I. KNO_3 lines (Fe$K\alpha_1$ radiation).

($hkil$)	2θ (KNO-I)	2θ (KNO-III)
$14\bar{5}0$	141.68	138.03
$32\bar{5}4$	133.85	131.81
$13\bar{4}4$	100.55	99.70
3, $\bar{1}$, $\bar{2}$, 10		97.96
$22\bar{4}0$	91.14	
1, 1, $\bar{2}$, 12	87.63	
$30\bar{3}6$	86.63	
$32\bar{1}8$	84.69	86.45

To heat the powder sample, a heated stage for the diffractometer, consisting of an aluminum sample dish on a lava heating stage, was constructed. Because of the large surface area of the sample, the temperature accuracy was estimated to be as poor as ±1°C. A second source of error in d is the absolute-angle measurement, as the diffractometer measures peaks on only one side of $\theta=0°$. To minimize this effect and the possible distortion of the heated sample stage, a small amount of Si powder was added to the KNO_3 sample to serve as an internal standard. The reference lattice parameter of Si, $a=5.43075$ Å at 25°C, and the thermal coefficient of expansion, $\alpha=2.6\times10^{-6}$ referred to 25°C, were determined by Straumanis *et al.*[11]

The KNO_3 samples were prepared with powders obtained from pulverized crystals grown from water solution and also from crystals grown from the molten state. Only powder which passed through 325 mesh was used. Before each temperature run, the samples were heated overnight at 100°C to remove any excessive moisture.

The measured 2θ values for KNO_3 were corrected by the deviation of the measured Si lines from their expected positions. As the Si lines are no more than 5° (in 2θ) from any KNO_3 lines, this procedure satisfactorily compensates for any sample stage distortions, as well as errors in absolute-angle measurements.

The lattice parameters, a and c, of the KNO_3 hexagonal unit cell were derived from the corrected 2θ values by the standard least-squares technique described by Cullity.[12] A computer program was used to evaluate the data for both $\cos^2\theta$ and $\cos\theta\cot\theta$ extrapolations. The resulting difference between the two procedures was negligible (one part in 5000).

The KNO_3 lines used in the determination of the lattice parameters are listed in Table I. They are indexed

[7] Y. Shinnaka, J. Phys. Soc. Japan **17**, 820 (1962).
[8] T. Yanagi, J. Phys. Soc. Japan **20**, 1351 (1965).
[9] U. Kawabe, T. Yanagi, and S. Sawada, J. Phys. Soc. Japan **20**, 2059 (1965).
[10] A. J. C. Wilson, J. Sci. Instr. **27**, 321 (1950).
[11] M. E. Straumanis, P. Borgeaud, and W. J. James, J. Appl. Phys. **32**, 1382 (1961).
[12] B. D. Cullity, *Elements of X-Ray Diffraction* (Addison-Wesley Publishing Company, Reading, Massachusetts, 1956).

TABLE II. Comparison of measurements.

	Fischmeister[a]	Kawabe[b]	Present measurement
a. Lattice parameter at 152°C			
a (Å)	5.423		5.420
c (Å)	9.638	9.75	9.761
ρ (g/cm³)	2.051	2.04	2.020
		$\rho_{measured}$[c] 2.021	
b. Change in volume at transition			
$\Delta\left(\frac{1}{\rho}\right)$ (cm³/g)		0.011	0.01554
		$\Delta\left(\frac{1}{\rho}\right)^{d}_{measured}=0.01425$	

[a] See Ref. 13.
[b] See Ref. 9.
[c] See Ref. 14.
[d] See Ref. 2.

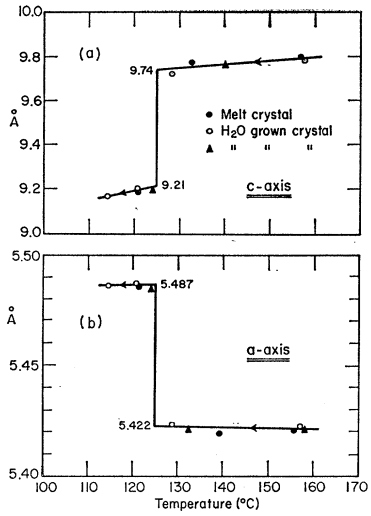

FIG. 2. The lattice parameters of KNO_3 near its ferroelectric transition. (a) c axis; (b) a axis of the hexagonal unit cell.

on the hexagonal unit cell for the calcite structure whose c axis is twice that of the KNO_3 hexagonal unit cell.

The temperature dependences of the lattice parameters calculated from the corrected KNO_3 lines are shown in Figs. 2(a) and 2(b).

A comparison of these results with previously measured lattice parameters of KNO_3 is given in Table II. Both Fischmeister[13] and Kawabe[9] used 2θ in the 40–50° range. The densities were measured by Cohen and Bredee.[14]

The internal consistency of the indexing of the measured KNO_3 lines was checked by comparing the resultant a and c values for each line given the extrapolated a/c ratio. The maximum deviation occurs in the ferroelectric phase and was approximately -0.003 Å for an a of 5.487 Å and -0.005 Å for a c of 9.20 Å. The error in our measurement was estimated to be one part per thousand. Within the accuracy of the experiment, the density predicted on the basis of these measurements agrees with the measured values.

IV. INTERPRETATION OF THE CHANGE IN LATTICE PARAMETER

The change in the lattice parameters of KNO_3 as it passes from the paraelectric to the ferroelectric phase is unusual in both magnitude and direction. The c axis contracts by ~5% and the a axis expands by ~1%.[15] This change appears to be the result of an ordering of permanent dipoles. When the dipoles are aligned in the ferroelectric phase, the additional Coulomb forces cause the lattice to contract along the ferroelectric axis.

Phenomenologically we interpret this lattice distortion as an electrostriction effect associated with the appearance of spontaneous polarization in the ferroelectric phase. The phenomenological equation[16] which describes the electrostriction effect is

$$\epsilon_i = s_{ij}\sigma_j + Q_{ikl}P_kP_l, \tag{3}$$

where ϵ_i is the strain, σ_j is the stress, and Q_{ikl} is the electrostriction coefficient. Assuming that the distortion occurs only through tensile strains, we obtain the following values for the electrostriction coefficients of KNO_3:

$$Q_{133}=\Delta a/aP_s^2=1.33\times10^{-11}\ \text{cm}^2/\text{dyn}, \tag{4}$$

$$Q_{333}=\Delta c/cP_s^2=-6.05\times10^{-11}\ \text{cm}^2/\text{dyn}, \tag{5}$$

where we have used $P_3=P_s=10\ \mu\text{C/cm}^2$ as determined from pyroelectric measurement.[6] $P_1=P_2=0$ and all other Q's are zero because of crystal symmetry. It may be noted that these values are opposite in sign to that of $BaTiO_3$ and two orders of magnitude greater.

If these values are employed in Devonshire's equation for the dependence of the transition temperature on hydrostatic pressure, one obtains good agreement with experiment. Following a deviation similar to Devonshire's,[16]

$$\frac{dT_c}{dp}=\frac{-(Q_{333}+2Q_{133})}{4\pi/C}=1.54\times10^{-8}\ ^\circ\text{C}/(\text{dyn/cm}^2), \tag{6}$$

[13] H. F. Fischmeister, J. Inorg. Nucl. Chem. **3**, 182 (1956).
[14] E. Cohen and H. L. Bredee, Z. Phys. Chem. **A140**, 391 (1929).
[15] In $BaTiO_3$, the well-known ferroelectric with a first-order transition, the behavior of the lattice is reversed. The ferroelectric axis expands and the perpendicular direction contracts as it undergoes the ferroelectric transition. $BaTiO_3$ is a so-called displacive-type ferroelectric. The Ti ions, which are the main agent of ferroelectricity in this crystal, are in oscillatory motion in the paraelectric phase. Kinase and Takahashi [J. Phys. Soc. Japan **10**, 942 (1955)] have pointed out that physically the expansion of the ferroelectric axis occurs at the transition to permit more room in the unit cell for the displacement of the Ti ion in the feroelectric phase of $BaTiO_3$.
[16] A. F. Devonshire, in *Advances in Physics*, edited by N. F. Mott (Taylor and Frances, Ltd., London, 1954), Vol. 3, p. 85.

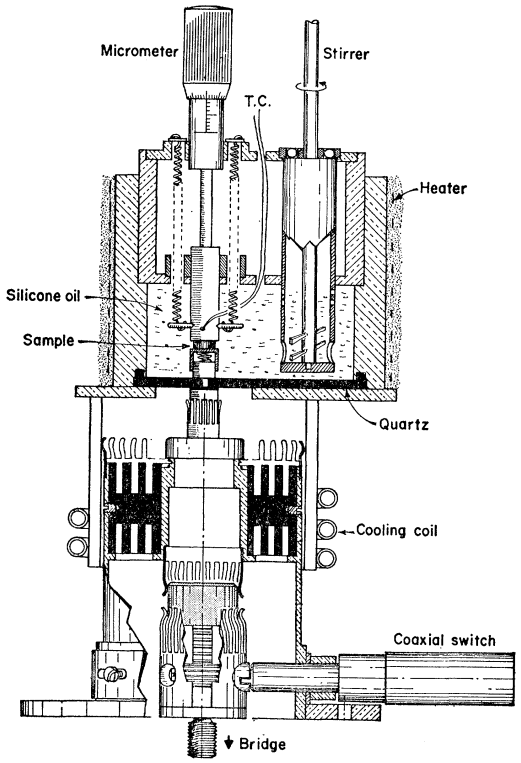

FIG. 3. Low-frequency (100 Hz-40 MHz) heated coaxial sample holder.

where $4\pi/C=2.23\times10^{-3}$ °K,[6] and C is the Curie constant. As measured by Bridgman,[2]

$$\frac{dT_c}{dp}=2.22\times10^{-8}\ ^\circ\mathrm{C}/(\mathrm{dyn/cm^2}).$$

The agreement is good in that the electrostriction effect predicts a linear pressure dependence for T_c and gives the magnitude of this dependence.

V. DIELECTRIC MEASUREMENTS

A. Low-Frequency Measurements

A coaxial sample holder for measuring the dielectric constant of a small disk sample was constructed to be used on the wide-range Schering bridge designed by Westphal.[17] It is shown in Fig. 3. The holder was filled with silicone oil to maintain a good thermal bath. The bottom electrode was spring-loaded so that the dielectric constant of the crystal is measured at zero stress. The holder was calibrated with a fused quartz sample as a standard. The highest frequency at which the inductive effects were negligible is approximately 40 MHz.

KNO_3 crystals were grown from a water solution.[6] They were cut and polished to the desired size. The sample sizes ranged in thickness from 0.5 to 1 mm and in area from 30 to 120 mm². The c axis was oriented perpendicular to the sample face within 1°. Because the crystal cracks in the Phase III → II reconstructive transformation, dielectric measurements were made on virgin crystals at all frequencies in the same temperature run.

The dielectric constants of KNO_3 at 10 kHz, 2 MHz, and 18 MHz are shown in Fig. 4(a). The dielectric losses at these frequencies in the paraelectric phase are shown in Figs. 4(b), 4(c), and 4(d). Unlike the molecular ferroelectric $NaNO_2$, there is no dielectric dispersion in KNO_3 at these low frequencies. The dielectric losses change from a positive to a negative temperature dependence as the frequency is increased from 10 kHz to 18 MHz. The conduction losses due to lattice defects are predominant at the low frequency, but the dielectric losses due to permanent dipoles become more important in the megacycle region.

The dielectric constants in the ferroelectric phase decrease with increasing frequency. This decrease is probably due to the partial clamping of the crystal by the piezoelectric effect in this phase, The ferroelectric phase did not appear for sample # 2, as this sample was not annealed up to 180°C.

The dielectric constant of KNO_3 has a typical Curie-Weiss behavior above the ferroelectric transition temper-

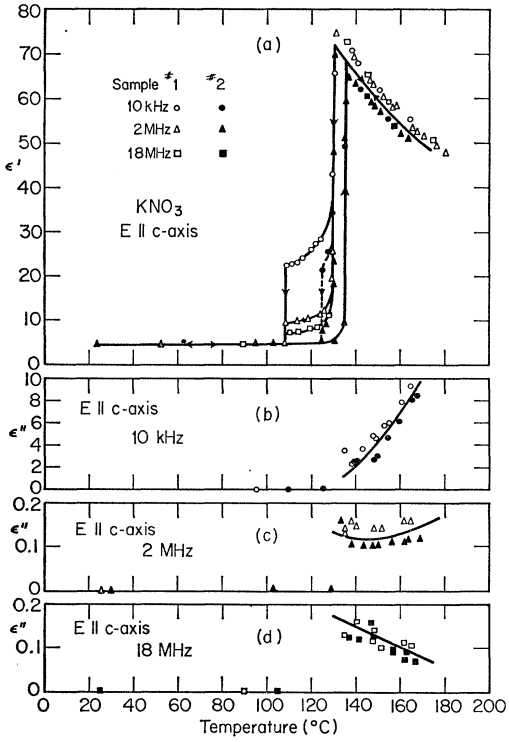

FIG. 4. Relative dielectric constants and losses of KNO_3 at 10 kHz, 2 MHz, and 18 MHz. (a) Dielectric constants; (b) dielectric losses at 10 kHz; (c) dielectric losses at 2 MHz; (d) dielectric losses at 18 MHz.

[17] W. B. Westphal, Insulation Research Laboratory, M.I.T. Technical Report No. 191, 1964, p. 49 (unpublished).

ature. The measured Curie constant is $C=6.1\times10^3$ °K and the extrapolated Curie temperature is $T_0=41$°C. These numbers are within 5% of the values reported by Yanagi.[9]

B. Microwave Coaxial Measurements

A disk sample in a coaxial line was used to determine the dielectric constants of KNO_3 at 1.5 GHz and at 3.0 GHz. The sample, of the same diameter as the inner conductor, was mounted at the end of a shorted coaxial line. In this geometry, in which the c axis of the crystal is parallel to the line, the disk approximates a parallel-plate capacitor. However, its capacitance must now be measured by transmission-line techniques. The theory of this measurement has been discussed by Westphal[18] and by Jaynes and Varenhorst.[19]

The coaxial slotted line was made from 15.9-mm i.d. copper pipe. The heated section at the end of the line was made of silver-plated thin-wall stainless steel to limit thermal conduction. Similarly, the center conductor was made of a silver-plated 2.75-mm o.d. thin-wall stainless tubing. It was also spring-loaded to assure good electrical contact to the disk sample. The slotted line was mounted vertically with the sample on top in order to limit heat loss and thermal gradients due to convection. The temperature gradient across the sample was less than 1°C. The thermal expansion of the line was 0.0856 mm/100°C.

The measuring technique was checked by measuring the dielectric constants of KRS-5 (42% TlBr, 58% TlI; $\epsilon=32.5$ at 10 MHz) single crystal and of ruby ($\epsilon=10.15$ at 100 kHz).[20] The measured dielectric constants on the coaxial slotted line were within 10% of the above values.

The single crystal of KNO_3 was shaped to the approximate size by a wet string saw. It was then mounted on the removable tip of the center conductor with silver paste and shaped to the final size (diam=2.75 mm and thickness=1.0 mm) by a polishing wheel made from #560 SiC polishing paper. The silver paste acts both as an adhesive and as the electrode of the disk sample.

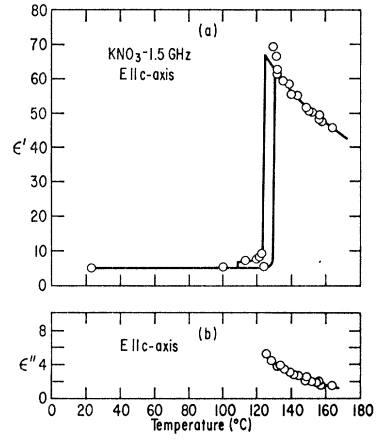

FIG. 5. Dielectric constants and losses of KNO_3 at 1.5 GHz. (a) Dielectric constants; (b) dielectric losses.

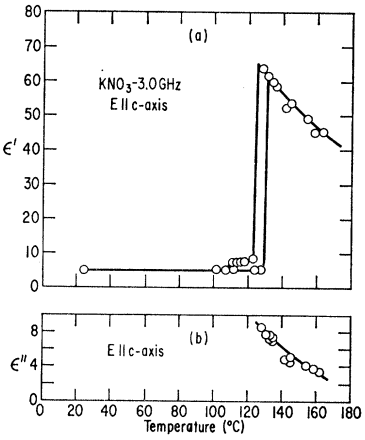

FIG. 6. Dielectric constants and losses of KNO_3 at 3.0 GHz. (a) Dielectric constants; (b) dielectric losses.

The dielectric constants of KNO_3 measured at 1.5 GHz and at 3.0 GHz are shown in Figs. 5(a) and (b), and 6(a) and (b). They were measured at both frequencies in the same initial temperature run. The dielectric constants of the paraelectric phase have decreased, and the dielectric losses have increased from the low-frequency values. This change appears to be the onset of dielectric relaxation in the paraelectric phase of KNO_3.

C. Microwave Perturbation Measurements

The dielectric constant of KNO_3 at 5.8 GHz and at 10.9 GHz were measured by cavity perturbation techniques. The effect of a small perturbation on the resonating frequency of a microwave cavity was first derived by Bethe and Schwinger[21] and by Slater.[22] This technique has been used by Kaminow and Harding to determine the dielectric constant at 9.2 GHz of KH_2PO_4.[23] If the dielectric sample perturbs only the electric field within the cavity, its relative complex dielectric constant, $\epsilon^*=\epsilon'-j\epsilon''$, is given by the following relations:

$$\epsilon'=B\frac{v_c}{v_s}\frac{\Delta f}{f}+1, \tag{7}$$

$$\epsilon''=\frac{B}{2}\frac{v_c}{v_s}\Delta\left(\frac{1}{Q}\right). \tag{8}$$

v_c and v_s are the cavity and sample volumes, respectively. Δf is the change in the resonating frequency f, and

[18] W. B. Westphal, in *Dielectric Materials and Applications*, edited by A. von Hippel (Technology Press, New York, 1954).
[19] E. T. Jaynes and V. Varenhorst, Stanford University, Stanford, California, Microwave Laboratory Report No. 287 (unpublished).
[20] *Table of Dielectric Materials* (M.I.T. Press, Cambridge, Massachusetts), Vols. IV and VI.
[21] H. A. Bethe and J. Schwinger, Cornell University, Ithaca, New York, NDRC Report No. D1-117, 1943 (unpublished).
[22] J. C. Slater, Rev. Mod. Phys. **18**, 441 (1946).
[23] I. P. Kaminow and G. O. Harding, Phys. Rev. **129**, 1562 (1963).

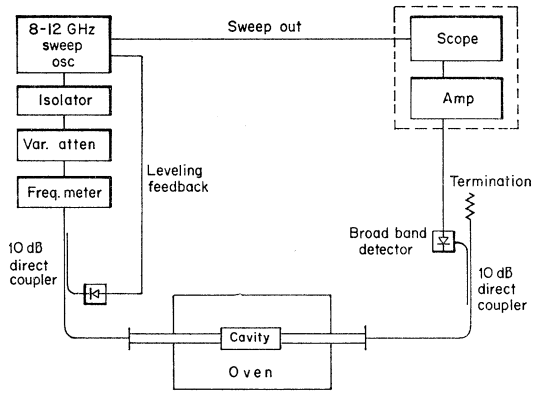

FIG. 7. Electronic system for measuring dielectric constants and losses by perturbation technique at x band.

$\Delta(1/Q)$ is the change in the loaded Q of the cavity. B is a constant determined by the cavity mode. It is 0.539 for the TM_{010} mode of a cylindrical cavity and is 0.500 for the TE_{103} mode of a rectangular cavity.

A cylindrical cavity operating in the TM_{010} mode was used at 5.8 GHz. The empty-cavity characteristics are: diam: 3.940 cm; height: 0.508 cm; volume: 6.18 cm^3; resonating frequency: 5.836 GHz at 25°C; 5.817 GHz at 180°C; Q: 2100 at 25°C; 1700 at 180°C; frequency change: -0.1225 MHz/°C.

The cavity at 10.9 GHz was constructed from half-height X-band waveguide operating in the TE_{103} mode. The empty cavity characteristics are: length: 5.000 cm; width: 2.286 cm; height: 0.508 cm; volume: 5.81 cm^3; resonating frequency: 10.931 GHz at 25°C; 10.900 GHz at 180°C; Q: 450 at 25°C, 480 at 180°C; frequency change: -0.193 MHz/°C.

The electronic system for the X-band measurement is shown in Fig. 7. The Q of the cavity was determined by measuring the half-power frequencies of the swept cavity characteristics. The precision variable attenuator was used to check the square-law response of the broad-band crystal detector. A similar coaxial system was used for 5.8 GHz except that the cavity was heated in a silicone oil bath.

Long thin crystals of KNO_3 with the c axis along their lengths were grown in approximately twenty-four hours by cooling a saturated solution of KNO_3. Clear sections of the needles were cut oversized and then partially dissolved in distilled water. The samples were clear and exhibited no detectable defects under microscopic examination with polarized light. Because the crystals had irregular cross sections, the sample volumes were determined by weight. The densities used were: 2.11 gm/cm^2 for Phase II and 2.02 gm/cm^3 for Phases I and III. Because of the reconstructive transformations in KNO_3, all measurements were made on virgin crystals.

In dielectric measurements, any gap that may occur between the crystal and its electrode may introduce a large error; the effect is akin to the addition of a capacitor in series with the sample. In such a case the resultant measured dielectric constants would be less than the true values. To eliminate this gap effect, one end of the samples was painted with silver paste. After curing at room temperature, the sample was attached to a copper rod with RTV silicone rubber. After the silicone rubber was cured, another coat of silver paste was applied to cover the silicone rubber and to electrically connect the original silver electrode to the copper rod. This copper rod filled the 1/16-in. hole in the cavity wall. To assure good contact to the opposite cavity wall, a small dab of silver paste was placed on the tip of the sample before it was inserted into the cavity. The cross-section view of a sample in the cavity is shown in Fig. 8. As the loss tangents of KNO_3 in the paraelectric phase are high ($\tan\delta > 0.2$), the presence of the silver paste would not introduce any appreciable error in our measurement.

Five samples were measured, three at 5.8 GHz and two at 10.8 GHz. The sample lengths ranged from 0.506 cm to 0.638 cm, and their volumes ranged from 1.23×10^{-3} to 2.69×10^{-3} cm^3. The average radius of the samples was about 0.2 to 0.3 mm. The results of the perturbation measurements are shown in Figs. 9 and 10. The dielectric constants of the paraelectric phase of KNO_3 have relaxed from the low-frequency values. Correspondingly, the dielectric losses have increased. The nature of the relaxation spectrum of KNO_3 will be discussed later.

The perturbation formulas (7) and (8) are valid if

$$\frac{\Delta f}{f} \ll 1 \tag{9}$$

and

$$(\Gamma R)^2 = \left\{\frac{2\pi R}{\lambda_0}\right\}^2 (\epsilon' - j\epsilon'') \ll 1, \tag{10}$$

where Γ is the complex propagational constant in the sample, R is the radius of the sample, and λ_0 is the free-space wavelength. If there is a slight curvature of the electric field within the sample, the first-order correction would be to increase v_s by the factor $1+(\Gamma R)^2/4$. For our measurements, $\Delta f_{\max} \sim 150$ MHz or $\Delta f/f < 0.026$ at 5.8 GHz, which satisfies (7). With an average radius of ~ 0.3 mm, the maximum correction at 10.8 GHz would be about 5% for $|\epsilon' - j\epsilon''| \sim 40$. No corrections were applied to our results.

There is a spread in our data of about 15 to 20%. However, at a given frequency the temperature depend-

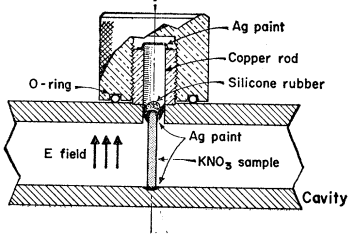

FIG. 8. Cross-sectional view of thin needle sample of KNO_3 in the cavity. c axis parallel to the $\mathbf{E}$ field.

ences of the dielectric constants of the samples are the same. The main error in this measurement is believed to be due to the uncertainty in the measured sample volumes and to the irregular cross-sectional areas of the samples.

Subsequent dielectric measurement of KNO_3 at 23.8 GHz showed that the averaged measured results at 10.9 GHz appears to be too low (approximately 20% lower than the expected value). The temperature dependence of the dielectric constants do agree with other measurements (see Fig. 13).

D. Microwave Standing-Wave Measurements

The dielectric constants of KNO_3 at 23.8 GHz was measured with a filled rectangular waveguide terminated by a shorting plate. The theory of measurement has been described by Westphal.[18]

A short section of K-band waveguide was heated in a small tubular heater. As the thin sample was in contact with the large shorting plate, the temperature gradient across the sample was small. The thermal expansion of the waveguide was 0.178 mm/100°C.

The sample of KNO_3 was cut from the a face of a crystal with a string saw and was polished to size on SiC polishing paper. Its cross-sectional dimensions fitted the waveguide very well. Its depth was 0.175 mm.

The measured dielectric constants and losses of KNO_3 at 23.8 GHz are shown in Figs. 11(a) and 11(b). They are almost independent of temperature. This behavior suggested that the dielectric relaxation spectrum is almost terminated at this frequency.

E. Far-Infrared Reflectivity Measurement

This measurement was undertaken to determine the upper frequency limit of ferroelectric behavior in KNO_3,

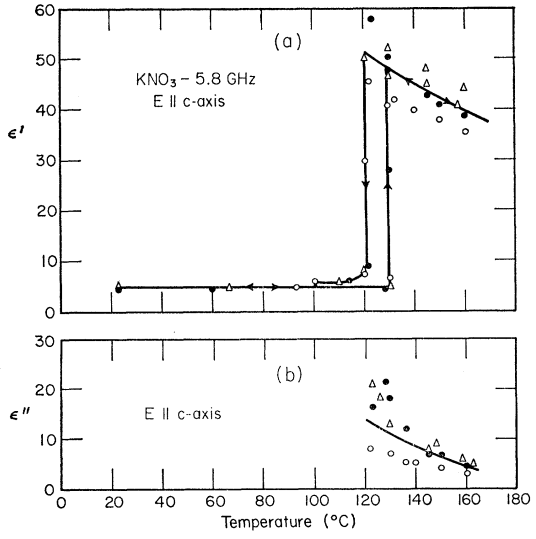

FIG. 9. Dielectric constants and losses of KNO_3 at 5.8 GHz. (a) Dielectric constants; (b) dielectric losses.

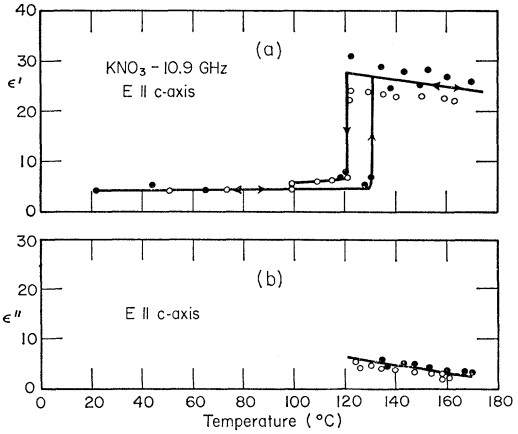

FIG. 10. Dielectric constants and losses of KNO_3 at 10.9 GHz. (a) Dielectric constants; (b) dielectric losses.

and to observe, if possible, lattice vibrations associated with the motion of the nitrate ion. The far-infrared lamellar-grating interferometer used in this investigation covered the spectral region from 12 to 100 cm^{-1}.[24] Reflection rather than transmission measurements were performed. To obtain detectable transmitted power, the sample must be less than 0.2 mm thick; with this thickness, interference effects make interpretation of the data difficult.

The reflection sample holder with 10°-angle-of-incident optics was constructed by Ballantyne.[25] The samples were a-face KNO_3 crystals grown from water solution. The reflectivities of the unpolarized radiation were nearly the same at 24 and at 146°C [flat at (15±3)% across the entire spectrum]. It may be inferred from these results that there is no well-defined lattice vibration in the spectral region 12 to 100 cm^{-1}. In particular, the transverse optical mode associated with the wave vector along the c axis is not observed in this spectral region. If we assume negligible loss, the average relative dielectric constant of a-face KNO_3 is about 4 to 6, the same as the static dielectric constant of Phase II.

F. Dielectric Spectra of Potassium Nitrate

The measured dielectric constants and losses along the c axis of the paralectric phase of KNO_3, plotted as a Cole-Cole diagram for different temperatures above the transition, are shown in Fig. 12. We have used $T-T_c$ as the temperature parameter because the ferroelectric transition occurs at a slightly different temperature for each experimental setup. The dielectric spectrum at a given temperature is of a relaxation type, and its occur-

[24] J. M. Ballantyne, M.I.T. Technical Report No. 188, 1964 (unpublished). S. J. Allen, Jr., M.I.T. Progress Report No. XXXI, p. 74, 1962 (unpublished); S. J. Allen, Jr., and J. M. Ballanytyne, M. I. T. Progress Report No. XXXII, p. 72, 1963 (unpublished).

[25] J. M. Ballantyne, Phys. Rev. **136**, A429 (1964).

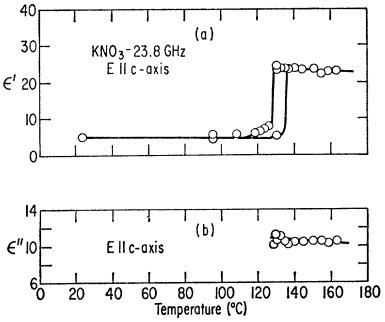

FIG. 11. Dielectric constants and losses of KNO_3 at 23.8 GHz. (a) Dielectric constants; (b) dielectric losses.

rence in the microwave region is usually associated with the existence of permanent dipoles in the solid.

A distributed relaxation spectrum is expected since the interaction among the permanent dipoles is strong in a ferroelectric cyrstal. The dielectric spectra of KNO_3, as shown in Fig. 12, fits the Cole-Cole distribution fairly well. The parameter, $(1-\alpha)$, of the distribution function

$$\frac{\epsilon-\epsilon_\infty}{\epsilon_s-\epsilon_\infty}=\frac{1}{1+(i\omega\tau)^{1-\alpha}} \tag{11}$$

varies from 0.57 to 0.52 for $T-T_c$ from 0°C to 40°C. Here ϵ_s and ϵ_∞ are the static and the optical dielectric constants, respectively; τ is the relaxation time and ω is the angular frequency.

On the basis of a model of an order-disorder arrangement of charged ions in double potential wells, Mason has predicted a single Debye relaxation time proportional to $1/(T-T_c)$ for Rochelle salt.[26] Hill and Ichiki were able to fit the measured dielectric constants of triglycine sulfate to a distributed relaxation spectra in which the relaxation time was also proportional to $1/(T-T_c)$.[27] For KNO_3, in which the ferroelectric transition is first order, the expected temperature dependence of the relaxation time would be $1/(T-T_0)$, where T_0 is the extrapolated Curie temperature. Following Hill and Ichiki, we have plotted the normalized dielectric constant, $(\epsilon'-\epsilon_\infty)/(\epsilon_s-\epsilon_\infty)$, versus $f/(T-T_0)$ as shown in Fig. 13. From the 3 dB point of this plot, we obtain for the relaxation time,

$$\tau=\frac{5.3\times10^{-9}}{T-T_0}\ \text{sec},$$

with $T-T_0$ in °K. For $\omega\tau\gg1$, Eq. (11) becomes

$$\ln\left(\frac{\epsilon'-\epsilon_\infty}{\epsilon_s-\epsilon_\infty}\right)\propto-(1-\alpha)\ln\omega\tau. \tag{12}$$

The value of $(1-\alpha)$, as determined from Fig. 13, is approximately 0.6.

[26] W. P. Mason, *Piezoelectric Crystals and Their Application to Ultrasonics* (D. Van Nostrand, Inc., New York, 1950).
[27] R. M. Hill and S. K. Ichiki, Phys. Rev. **128**, 1140 (1962).

VI. DISCUSSION

A. Relation to Cochran's Theory of Ferroelectricity

Cochran's[28] theory is based on the generalized Lyddane-Sachs-Teller (LST) relation which relates the lattice vibrations to the dielectric constants of a crystal. For a diatomic crystal,

$$\frac{\epsilon_s}{\epsilon_\infty}=\frac{\omega_L^2}{\omega_T^2}, \tag{13}$$

where ω_L and ω_T are the longitudinal and transverse optical lattice vibrations in the long-wavelength approximation. Cochran and Cowley have shown that, if the adiabatic, electrostatic, and harmonic approximations are valid for lattice dynamics, the LST relation is valid for crystals of any symmetry.[29]

Ferroelectricity could occur in a crystal if a softening of the transverse optical mode takes place by the balancing of the long-range Coulombic forces against the short-range repulsive forces within the crystal.[28] In addition, if the short-range forces are slightly anharmonic, ω_T could depend on temperature in the following way:

$$\omega_T\sim(T-T_0)^{1/2}. \tag{14}$$

Since ω_L is, in general, temperature-independent, ϵ_s has a Curie-Weiss behavior, $\epsilon_s\sim1/(T-T_0)$.

If Cochran's theory is applicable to KNO_3, the expected ω_T for KNO_3 I can be calculated from ϵ_s:

$$\begin{aligned}\omega_T^2&=\omega_L^2\epsilon_\infty/\epsilon_s\\&=\omega_L^2\epsilon_\infty(T-T_0)/C,\end{aligned} \tag{15}$$

where $\epsilon_s=C/(T-T_0)$ with $C=6\times10^3$ °K and $T_0=40$°C as the experimentally determined parameters. At the ferroelectric transition of KNO_3, $T-T_0=90$°K. If we assume that ω_L has a low but reasonable value of 100 cm^{-1} and $\epsilon_s=5$, then we expect $\omega_T=28$ cm^{-1}. We did not observe such a vibration in the far-infrared spectra of paraelectric KNO_3. The observed dielectric dispersion occurs at about 10 GHz (0.3 cm^{-1}). Because of this large discrepancy between theory and experiment, one must

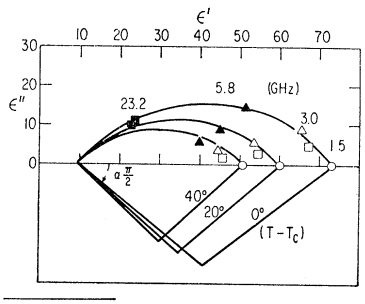

FIG. 12. Dielectric dispersion of the paraelectric phase of KNO_3 plotted as a Cole-Cole diagram; $(1-\alpha)=0.57$ to 0.52 for $T-T_c=0$–40°C.

[28] W. Cochran, in *Advances in Physics*, edited by N. F. Mott (Taylor and Frances, Ltd., London, 1960), Vol. 9, p. 387.
[29] W. Cochran and R. A. Cowley, J. Phys. Chem. Solids **23**, 447 (1962).

conclude that Cochran's theory, as it stands, does not apply to KNO_3.

Cochran's theory should not be considered universally applicable to ferroelectrics. He explicitly noted that his theory may not be valid in describing the dielectric properties of a material exhibiting an order-disorder transformation.[28] This should be evident because the LST relation, the foundation of the theory, is based on the validity of the harmonic approximation as well as the periodicity of the lattice. The accuracy of the LST relation in relating the lattice dynamics of a completely disordered lattice to the dielectric constants of the crystal is doubtful.

B. Physical Model of Ferroelectricity in KNO_3

The experimental evidence presented herein—the contraction of the ferroelectric axis at the paraelectric-to-ferroelectric phase transition, and the relaxation type of dielectric dispersion of the paraelectric phase—all suggests that ferroelectricity in KNO_3 is due to the ordering of permanent dipoles. The permanent dipole moment in the paraelectric phase is believed to be due to the displacement of the nitrate ion from the center of the unit cell. The structure analysis by Tahvonen[3] has suggested that the amplitude of oscillation of this ion is about 0.4 Å along the c axis. If we consider instead that the structure is a disorder array of nitrate ions displaced from the center of the unit cell by 0.4 Å, the dipole moment per unit cell would be 9.8 $\mu C/cm^2$ [as evaluated from Eq. (1) and the measured lattice parameters]. This value is very close to the measured spontaneous polarization of the ferroelectric phase.

The most reasonable model to account for the displacement of the nitrate ion is a double potential well along the c axis of KNO_3 I. The potential hill at the center of the unit cell prevents free oscillation of the nitrate ion. The dipole moment can reverse direction by jumping from one well to another via a thermally-activated process.[30] Because the dipole moment is due to the displacement of a heavy charged ion from the center of the unit cell, the dipole is intimately linked to the lattice.

The lattice-dipole coupling is very strong, as exhibited by the large electrostriction effect in KNO_3-I. Any distortion of the lattice would affect the dipole moment by changing the displacement or by changing the volume. Conversely, any change in dipole moment would affect the lattice. As we shall show, this lattice-dipole coupling is responsible for the observed first-order ferroelectric transition in KNO_3 even though the transition is an order-disorder phenomenon.

It may be pointed out here that this lattice-dipole coupling is not peculiar to ferroelectrics. Bean and Rodbell have suggested that the lattice-magnetic dipole coupling is responsible for the observed first-order magnetic transition in MnAs.[31] An intuitive description on how the lattice dipole coupling can give rise to a first-order transition for an order-disorder phenomenon has been given by Bean and Rodbell.

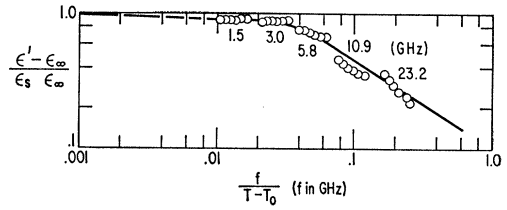

FIG. 13. $\text{Log}(\epsilon'-\epsilon_\infty/\epsilon_s-\epsilon_\infty)$ of KNO_3 versus $\log(f/T-T_0)$.

Recently Yanagi has treated the problem of ferroelectric interaction in KNO_3 based on a point dipole model.[8] His treatment parallels Slater's calculation for $BaTiO_3$ in which the correction terms to the Lorentz internal field were applied to find the necessary ionic polarizability for the "$4\pi/3$ catastrophe."[32] The applicability of the point-dipole model to KNO_3 is rather dubious for the following reason: Slater showed that in $BaTiO_3$ the required Ti ionic polarizability for the "$4\pi/3$ catastrophe" is only about 10% of the total electronic polarizability because of the correction terms to the Lorentz internal field. Without these correction terms, the required ionic polarizability would be over 50% of the total electronic polarizability—an unreasonably large number. Yanagi's results indicate that, with the correction terms, the required ionic polarizability for NO_3^- is about 300% of the total electronic polarizability—a most unreasonably large number.

Yanagi also found that with the correction to the Lorentz internal field for the rhombohedral unit cell, the dipole interaction is maximum at the rhombohedral angle between 70 and 80°. As the measured rhombohedral angle of KNO_3 at the ferroelectric transition is about 74°, Yanagi concluded that the transition occurs at this angle because the dipole interaction is at a maximum. He also pointed out that $CaCO_3$, with a rhombohedral angle of 75°, is not ferroelectric. We note that using the electronic polarizability for Ca^{++} and for CO_3^{--} as given by Tessman, Kahn, and Shockley,[33] the required ionic polarizability of CO_3^{--} for "$4\pi/3$ catastrophe "to occur in $CaCO_3$ is 10.4 to 12.9×10^{-24} cgs units—slightly smaller than Yanagi's calculated ionic polarizability for NO_3^- in KNO_3, which is 13.0 to 13.6×10^{-24}. Thus, based on the point-dipole model alone, there is no reason why $CaCO_3$ would not be ferroelectric.

We have treated the problem of a ferroelectric transition of ordered-disordered dipoles by assuming the existence of an internal field. The lattice-dipole coupling has been attributed to the lattice dependence of this

[30] H. Frohlich, *Theory of Dielectrics* (Oxford University Press, London, 1949).

[31] C. P. Bean and D. S. Rodbell, Phys. Rev. **126**, 104 (1962).
[32] J. C. Slater, Phys. Rev. **78**, 749 (1950).
[33] J. R. Tessman, A. H. Kahn, and W. Shockley, Phys. Rev. **92**, 890 (1953).

internal field. The resultant statistical and thermodynamic theory shows that it is primarily the elastic and the electrostrictive properties of the crystal that determine the ferroelectric transition temperature of KNO_3.

VII. STATISTICAL THEORY OF FERROELECTRICITY IN KNO_3

A model of ferroelectricity based on the order-disorder arrangement of a charged ion in two equilibrium positions has been treated by Devonshire.[16] We shall adapt his treatment to KNO_3, but shall neglect electronic–electronic dipole and electronic–ionic dipole interactions. For a system of N dipoles, each of dipole moment $\mu=q\delta$, the free energy A is

$$A=U-TS, \tag{16}$$

where

$$S=k\ln\left[\frac{N!}{[\frac{1}{2}N(1+x)]![\frac{1}{2}N(1-x)]!}\right]$$
$$\simeq-\tfrac{1}{2}kN[(1+x)\ln(1+x)+(1+x)\ln(1-x)-2\ln 2] \tag{17}$$

is the configuration entropy of these dipoles and where

$$U=-\tfrac{1}{2}\gamma P^2 \tag{18}$$

is the electrostatic energy of this system of dipoles. $x=P/N\mu$ is the long-range ordering parameter and γ is the interaction constant between the dipoles. This form of the electrostatic interaction between dipoles is equivalent to the assumption of an internal field

$$E_i=E_a+\gamma P. \tag{19}$$

E_a is the applied field. This assumption is in the spirit of the usual local-field theory of ferromagnetism inasmuch as the polarization is due to permanent rather than point dipoles.

The free energy A implicitly assumes a rigid lattice. To account for the possible distortion of the lattice, the free energy must now include the strain energy of the crystal:

$$A'=U-TS+\tfrac{1}{2}c_{ij}\epsilon_i\epsilon_j, \tag{20}$$

where

$$\tfrac{1}{2}c_{ij}\epsilon_i\epsilon_j=(c_{11}+c_{12})\epsilon_1^2+\tfrac{1}{2}c_{33}\epsilon_3^2+2c_{13}\epsilon_1\epsilon_3. \tag{21}$$

As in Sec. IV, we have assumed that the distortion occurs only through the tensile strain. This assumption is reasonable in view of the agreement between the predicted and the measured pressure dependence of the transition temperature.

To account for the lattice dipole coupling, we assume γ to be of the following form:

$$\gamma=\gamma_0[1+\beta_c\epsilon_3+\beta_a\epsilon_1]$$
$$=\gamma_0\left[(1+\beta_c)\left\{\frac{c-c_0}{c_0}\right\}+\beta_a\left\{\frac{a-a_0}{a_0}\right\}\right]. \tag{22}$$

a and c are the lattice parameters of the crystal; a_0 and c_0, of a reference state. This assumption is based on the nature of the lattice-dipole coupling as described in Sec. VI B.

At equilibrium, a and c are determined by

$$\frac{\partial A'}{\partial a}=2(c_{11}+c_{12})\epsilon_1+2c_{13}\epsilon_3-\tfrac{1}{2}\gamma_0\beta_aP^2=0, \tag{23}$$

$$\frac{\partial A'}{\partial c}=2c_{13}\epsilon_1+c_{33}\epsilon_3-\tfrac{1}{2}\gamma_0\beta_cP^2=0. \tag{24}$$

Solving for ϵ_1 and ϵ_2 we obtain

$$\epsilon_1=\gamma_0[c_{33}\beta_a-2c_{13}\beta_c]P^2/D, \tag{25}$$

$$\epsilon_3=\gamma_0[2(c_{11}+c_{12})\beta_c-2c_{13}\beta_a]P^2/D, \tag{26}$$

where $D=c_{33}(c_{11}+c_{12})-2c_{13}^2$.

Comparing Eqs. (25) and (26) with Eqs. (4) and (5), we find that the electrostriction coefficients are given by:

$$Q_{133}=\gamma_0[c_{33}\beta_a-2c_{13}\beta_c]/D, \tag{27}$$

$$Q_{333}=\gamma_0[2(c_{11}+c_{12})\beta_c-2c_{13}\beta_a]/D. \tag{28}$$

According to Eqs. (21) and (22), the electrostriction effect in KNO_3 is a manifestation of the lattice dependence of the internal field.

To see how the above theory can predict a first-order ferroelectric transition and to relate the theory to the thermodynamic theory, we expand the free energy A' as a function of the polarization. The tensile strains in coupling to the dipoles are determined by Eqs. (25) and (26). Substituting these equations into A', expanding TS for small x, and keeping only the P-dependent terms, we obtain

$$A'=\tfrac{1}{2}\eta'P^2+\tfrac{1}{4}\xi P^4+\tfrac{1}{6}\rho'P^6+\cdots, \tag{29}$$

where

$$\eta'=\frac{4\pi}{C}(T-T_0), \tag{29a}$$

$$\frac{4\pi}{C}=\frac{kN}{(N\mu)^2}, \tag{29b}$$

$$T_0=\gamma_0\left(\frac{C}{4\pi}\right), \tag{29c}$$

$$\xi=\xi'-2\lambda', \tag{29d}$$

$$\xi'=\frac{T}{3}\left(\frac{4\pi}{C}\right)\left(\frac{1}{N\mu}\right)^2, \tag{29e}$$

$$\rho'=\frac{T}{5}\left(\frac{4\pi}{C}\right)\left(\frac{1}{N\mu}\right)^4, \tag{29f}$$

and

$$\lambda' = -2(c_{11}+c_{12})Q_{133}^2 + c_{33}Q_{333}^2 + 4c_{13}Q_{133}Q_{333} + \beta_3 Q_{333} + \beta_1 Q_{133}. \quad (29g)$$

If we did not include the strain energy of the crystal and the possibility of lattice-dependent internal fields, λ' would be zero and the resultant free energy would be

$$A = \tfrac{1}{2}\eta' P^2 + \tfrac{1}{4}\xi' P^4 + \tfrac{1}{6}\rho' P^6 + \cdots. \quad (30)$$

Since $T>0$, $C>0$, and $N\mu>0$, and thus $\xi'>0$ and $\rho'>0$, the free energy A would result in a second-order transition, as expected for an order-disorder phenomenon.

By including the additional strain energy and the lattice-dipole terms in A', there is now a possibility of a first-order transition depending on the sign of ξ. If ξ is still positive, it means the lattice-dipole coupling is not strong enough to distort the lattice sufficiently for a first-order transition. On the other hand, ξ could become negative if the coupling were strong enough to distort the lattice and cause a discontinuous jump in the spontaneous polarization at the transition temperature. We shall relate the above theory with Devonshire's thermodynamic theory of ferroelectric transition and compare the theoretically predicted with the experimentally determined values.

VIII. THERMODYNAMIC THEORY OF FERROELECTRIC TRANSITION IN KNO_3

Devonshire has developed the thermodynamic theory of ferroelectric transition based upon the following free-energy function:

$$A(T,P)_{\sigma=0} = \tfrac{1}{2}\eta P^2 + \tfrac{1}{4}\xi P^4 + \tfrac{1}{6}\rho P^6, \quad (31)$$

with

$$\eta = \frac{4\pi}{C}(T-T_0).$$

It is similar to Eq. (30), but the stress is zero to match the usual experimental condition. The constants C and T_0 are chosen to match the measured Curie-Weiss dependence of the susceptibility in the paraelectric phase. The constants ξ and ρ can be determined, assuming they are temperature-independent, by matching the curve of spontaneous polarization versus temperature. Using the curve as determined by Sawada *et al.* from the pyroelectric measurement,[6] we obtain the values shown in Table III.

The transition temperature for a first-order ferroelectric transition is given by

$$T_c = T_0 + \frac{3}{16}\frac{C}{4\pi}\frac{\xi^2}{\rho}. \quad (32)$$

The resultant T_c calculated from the experimentally determined values of $4\pi/C$, ξ, and ρ is shown in Table III.

TABLE III. Coefficients of the free-energy function $A(T,P) = (2\pi/C)(T-T_0) + \frac{1}{4}\xi P^4 + \frac{1}{6}\rho P^6$.

	Experiment	Theory
$\frac{4\pi}{C}$ (°K)	2.23×10^{-3} [a]	1.85×10^{-3}
ξ (cm^4/esu^2)	-6×10^{-10} [b]	-20.9×10^{-10}
ρ (cm^9/esu^4)	4×10^{-19} [b]	2.2×10^{-19}
ΔQ (cal/mole)	616[c]	605
T_c (°K)	T_0+90 [a]	$T_0+72.5$ [d]

[a] See Ref. 6.
[b] Calculated from the pyroelectric data of Ref. 6.
[c] See Ref. 2.
[d] Calculated from the measured ξ and ρ.

To calculate the coefficients of Devonshire's free energy, one must consider that while experimentally the dielectric properties of a crystal are measured at constant stress, theoretically the properties of a crystal are usually calculated by assuming a rigid lattice or at constant strain. With the externally imposed condition of zero stress, the strain in a ferroelectric crystal is no longer zero. One must transform the theoretically calculated free energy (at constant strain), $A'(T,\epsilon,P)$, to $A(T,P)_{\sigma=0}$. We have

$$A'(T,\epsilon,P) = A'(T,P) + \tfrac{1}{2}c_{ij}\epsilon_i\epsilon_j + q_{ikl}\epsilon_i P_k P_l, \quad (33)$$

where $A'(T,P)$ is the theoretically calculated free energy at constant strain. The second term on the right-hand side is the elastic energy of the crystal, but now all strain terms are included. The last term is the coupling between the electrostriction effect and the polarization. This term would result from a power-series expansion of the free energy of a dielectric crystal (see Jona and Shirane[34]).

For trigonal crystals with $P_3=P$, and $P_1=P_2=0$, we have

$$\tfrac{1}{2}c_{ij}\epsilon_i\epsilon_j = \tfrac{1}{2}c_{11}(\epsilon_1^2+\epsilon_2^2) + c_{12}\epsilon_1\epsilon_2 + \tfrac{1}{2}c_{33}\epsilon_3^2 + c_{13}(\epsilon_1\epsilon_3+\epsilon_2\epsilon_3) + c_{14}(\epsilon_1\epsilon_4 - \epsilon_2\epsilon_4 + \epsilon_5\epsilon_6) + \tfrac{1}{2}c_{44}(\epsilon_4^2+\epsilon_5^2) + \tfrac{1}{4}(c_{11}-c_{12})\epsilon_6^2 \quad (34)$$

and

$$q_{ikl}\epsilon_i P_k P_l = q_{133}(\epsilon_1+\epsilon_2)P^2 + q_{333}\epsilon_3 P^2. \quad (35)$$

The conditions for zero stress are

$$\sigma_i = \frac{\partial A'(T,\epsilon,P)}{\partial \epsilon_i} = 0. \quad (36)$$

Solving the six equations for ϵ_i and using the relations

$$s_{ij}c_{jk} = \delta_{ik}, \quad (37)$$

$$Q_{ikl} = -s_{ij}q_{jkl}, \quad (38)$$

we obtain

$$\epsilon_3 = Q_{333}P^2, \quad \epsilon_1 = \epsilon_2 = Q_{133}P^2, \quad (39)$$

with

$$\epsilon_4 = \epsilon_5 = \epsilon_6 = 0.$$

[34] F. Jona and G. Shirane, *Ferroelectric Crystals* (The Macmillan Company, New York, 1962).

These results verify our assumption that the lattice distorts through the tensile strain only.

We must now select a model to calculate $A'(T,P)$. If the model is that of the order-disorder arrangement of charged ions in double potential wells, then $A'(T,P)=A$ as given by Eq. (30) of the last section. Substituting Eq. (30) and the strains of Eq. (39) into $A'(T,\epsilon,P)$, we obtain

$$A'(T,\epsilon,P)_{\sigma=0}=\tfrac{1}{2}\eta' P^2+\tfrac{1}{4}(\xi'-2\lambda)P^4+\tfrac{1}{6}\rho' P^6, \quad (40)$$

where

$$\lambda=2(c_{11}+c_{12})Q_{133}^2+4c_{13}Q_{133}Q_{333}+c_{33}Q_{333}^2, \quad (41)$$

and by comparing Eq. (40) with Eq. (31), we have

$$\eta=\eta', \quad \rho=\rho' \quad \text{and} \quad \xi=\xi'-2\lambda.$$

An order of magnitude of the correction term λ may be obtained if we use the elastic constants of $NaNO_3$. The constants are not available for KNO_3-I, but the two crystals have similar crystal structure and thermal coefficients of expansion. Using the constants for $NaNO_3$,[35]

$$c_{11}=8.67, \quad c_{33}=3.74, \quad c_{12}=1.63, \quad c_{13}=1.60 \quad (\times 10^{11}\ \text{dyn/cm}^2),$$

and the electrostriction coefficients of KNO_3, the correction term to ξ' is

$$2\lambda=24.2\times 10^{-10}\ \text{cm}^2/\text{dyn}.$$

Using $T\simeq T_c=398°\text{K}$, $N\mu=10\ \mu\text{C/cm}^2$, the measured lattice parameters, and Eqs. (29b), (29e), and (29f), we obtain the theoretical values of $4\pi/C$, ξ, and ρ shown in Table III. The latent heat of transition is larger than

$$\frac{2\pi}{C}T_c(\Delta P_s),$$

because of the temperature dependence of ξ' and ρ'. It is

$$\Delta Q=\frac{2\pi}{C}\left(1+\tfrac{1}{6}+\frac{1}{15}\right)T_c(\Delta P_s)^2 \quad (42)$$
$$=605\ \text{cal/mole}.$$

The agreement between theory and experiment is good, considering the approximations involved in the theory. The negative value of ξ predicts the observed first-order transition in KNO_3. One would expect the elastic constant of KNO_3 to be less than that of $NaNO_3$. If so, the agreement between $\xi'-2\lambda$ and the measured ξ would be better.

As calculated from the statistical theory in Sec. VII, the coefficient of the P^4 term in Eq. (29) would give the same results as above. If the electrostriction coefficients as related to β_a and β_c by Eqs. (27) and (28) are substituted into λ, then $\xi'-2\lambda'=\xi'-2\lambda$.

The statistical and the thermodynamic theories are the same in that both assume an order-disorder model of permanent dipoles. The theories are different in that the statistical theory gives a microscopic explanation for the electrostriction effect which is treated phenomenologically in the thermodynamic theory.

IX. THE EFFECT OF THE SUBSTITUTION OF Rb^+ FOR K^+

The effect of the substitution of Rb^+ and NH_4^+ for K^+ has been studied by Yanagi and Kawabe.[36,37] The effect of NH_4^+ substitution is complex because the nonspherical nature of this ion changes many properties other than the dielectric properties of the crystal. For instance, the ferroelectric phase in $K_{1-x}(NH_4)_xNO_3$ system becomes stable (for $x>0.2$) and has a wider temperature range at atmospheric pressure. The effect of Rb^+ substitution can be understood in terms of the theory presented above. The ferroelectric phase of $K_{1-x}Rb_xNO_3$ is still metastable at atmospheric pressure, but the Curie constant C increases and T_c decreases with increasing x.

The elastic properties of KNO_3 are the most important factor in determining the transition temperature. Its effect on T_c is given by

$$\Delta T_c=-\frac{C}{4\pi}\left(\frac{3\xi}{4\rho}\right)\Delta\lambda \quad (43)$$

[from Eq. (32)].

The measurements of Kawabe[9] showed that the relative lattice distortion at the transition and the spontaneous polarization do not change much with small Rb^+ concentration; thus the main contribution to $\Delta\lambda$ would be the variation in the elastic constants. Substituting the values for the constants in Eq. (43), we see that a 1% decrease in the elastic constants of the crystal would result in a decrease of T_c by $\sim$0.4°C. For $K_{0.5}Rb_{0.5}NO_3$, $T_c\sim$90°C. This decrease of 35°C from T_c of KNO_3 would require only a 10% decrease in the elastic constants of the crystal. The large ionic radius of Rb^+ increases the lattice parameters and thus the molecular volume. As C is inversely proportional to the number of dipoles per unit volume (or proportional to the molecular volume), an increase in C would result from Rb^+ substitution.

X. CONCLUSION

From our measurements of the lattice distortion at the ferroelectric transition and of the dielectric dispersion in KNO_3-I, we concluded that ferroelectricity in KNO_3 is the ordering of permanent dipoles in which a strong lattice-dipole coupling causes the observed first-order ferroelectric transition. We have shown that a semiphenomenological statistical theory gives good agreement with experiments and predicts the anomalies

[35] J. Bhimasenachar, Proc. Indian Acad. Sci. **A41**, 72 (1955).

[36] T. Yanagi and S. Sawada, J. Phys. Soc. Japan **18**, 1228 (1963).

[37] U. Kawabe, T. Yanagi, and S. Sawada, J. Phys. Soc. Japan **19**, 767 (1964).

associated with the ferroelectric transition. The discrepancy between theory and experiment is probably due to the lack of a more sophisticated theoretical treatment which would treat the complete problem of lattice dynamics of a distortable disordered dipolar lattice.

ACKNOWLEDGMENTS

It is a pleasure to thank Professor R. E. Newnham and Dr. R. Santoro for making available the x-ray diffractometer, Professor D. J. Epstein and Dr. P. Cole for the use of the microwave equipment, and Professor P. A. Miles and Dr. S. J. Allen for the use of the far-infrared interferometer. The help of W. B. Westphal in making the low-frequency dielectric measurements and the critical reading of the manuscript by Professor F. Arntz are deeply appreciated. Computation was done at the Computation Center at the Massachusetts Institute of Technology, Cambridge, Massachusetts.

PHYSICAL REVIEW VOLUME 154, NUMBER 2 10 FEBRUARY 1967

Magnetoelectric Effect in Cr_2O_3 Single Crystal as Studied by Dielectric-Constant Method

H. B. LAL, RAMJI SRIVASTAVA, AND K. G. SRIVASTAVA
Physics Department, University of Allahabad, Allahabad, India
(Received 17 December 1965; revised manuscript received 11 August 1966)

An anomaly in the dielectric constant of a single crystal of Cr_2O_3 in the neighborhood of the Néel temperature is studied with and without external magnetic fields up to a maximum value of 19 kOe. It is observed that the absolute value of the apparent change in the dielectric constant at the Néel temperature increases linearly with applied magnetic field and has a tendency to become constant at fields higher than 17 kOe. This effect is discussed on the basis of structure-sensitive magnetoelectric effects arising from changes in the domain pattern. Rado's spin-orbit atomic model is also considered as a possibility.

I. INTRODUCTION

UNTIL recently, the subjects of magnetostatics and electrostatics were considered to be independent. Landau and Lifshitz[1] first pointed out that magnetoelectric (ME) effects may, in principle, exist in spin-ordered materials. Their arguments were based on thermodynamics and symmetry considerations, and did not invoke any atomic mechanism for this effect. Dzyaloshinskii[2] gave more detailed arguments along similar lines and showed, in particular, that magnetoelectric effects could be observed in single crystals of chromium oxide. While Astrov[3,4] experimentally observed $(ME)_E$ (magnetic polarization produced by the application of an external electric field), Rado and Folen[5–7] observed both $(ME)_E$ and $(ME)_H$ (electric polarization produced by the application of an external magnetic field) independently. Similar effects were observed for antiferromagnetic Ti_2O_3 also.[8] Recently magnetoelectric effects have been observed also for the Cr_2O_3-Al_2O_3 system[9] and for the ferromagnetic $Ga_{2-x}Fe_xO_3$ system.[10] Shtrikman and Treves[11] have shown the existence of a magnetoelectric effect in polycrystalline chromium oxide, produced by cooling the sample through the Néel temperature in the presence of electric and magnetic fields, both applied in the same direction. O'Dell[12] has used a pulsed-magnetic-field technique to measure the magnetoelectric effect in ceramic disks of chromium oxide and has mentioned the possibility of using magnetoelectric materials as memory-device elements which, as he points out, should be independent of frequency below the antiferromagnetic resonance frequency (about 100 kMc/sec).

An atomic mechanism for explaining magnetoelectric effects was put forward by Rado[13,14] and is based on the spin-orbit interaction. Phenomenologically, the situation may be described as follows. At temperatures below

[1] L. D. Landau and E. M. Lifshitz, *Electrodynamics of Continuous Media* (Addison-Wesley Publishing Company, Inc., Reading, Massachusetts, 1960), p. 119.
[2] I. E. Dzyaloshinkii, Zh. Eksperim. i Teor. Fiz. **37**, 881 (1959) [English transl.: Soviet Phys.—JETP **10**, 628 (1960)].
[3] D. N. Astrov, Zh. Eksperim. i Teor. Fiz. **38**, 984 (1960) [English transl.: Soviet Phys.—JETP **11**, 708 (1960)].
[4] D. N. Astrov, Zh. Eksperim. i Teor. Fiz. **40**, 1035 (1961) [English transl.: Soviet Phys.—JETP **13**, 729 (1961)].
[5] V. J. Folen, G. T. Rado, and E. W. Stalder, Phys. Rev. Letters **6**, 607 (1961).
[6] G. T. Rado and V. J. Folen, Phys. Rev. Letters **7**, 310 (1961).
[7] G. T. Rado and V. J. Folen, J. Appl. Phys. Suppl. **33**, 1126 (1962).
[8] V. I. Al'shin and D. N. Astrov, Zh. Eksperim. i Teor. Fiz. **44**, 1195 (1963) [English transl.: Soviet Phys.—JETP **17**, 809 (1963)].
[9] S. Foner and M. Hanabusa, J. Appl. Phys. **34**, 1246 (1963).
[10] G. T. Rado, Phys. Rev. Letters **13**, 335 (1964); in *Proceedings of the International Conference on Magnetism, Nottingham, 1964* (The Institute of Physics and The Physical Society, London, 1965).
[11] S. Shtrikman and D. Treves, Phys. Rev. **130**, 986 (1963).
[12] T. H. O'Dell, Phil. Mag. **10**, 899 (1964).
[13] G. T. Rado, Phys. Rev. Letters **6**, 609 (1961).
[14] G. T. Rado, Phys. Rev. **128**, 2546 (1962).